Electr Eng (2008) 90:323–330
DOI 10.1007/s00202-007-0088-9

ORIGINAL PAPER

Intelligent two-port numerical algorithm for transmission lines disturbance records analysis

Zoran Radojević · Vladimir Terzija

Received: 29 August 2007 / Accepted: 19 September 2007 / Published online: 16 October 2007

Abstract This paper presents a new intelligent numerical algorithm for analysis of transmission lines disturbance records. The algorithm improves the existing methodologies for fault location, adaptive autoreclosure, detailed disturbance records analysis, and fault data management. It is based on the processing of voltages and currents recorded at both of the line terminals. The algorithm does not require synchronized sampling of data from the line terminals. The proposed algorithm is derived in the spectral domain and is based on the application of the discrete Fourier transform. In the algorithm development, the fault arc is included in the complete fault model. One of advanced algorithm features is ability to determine both the arc and the fault/tower-footing resistance. The algorithm is thoroughly tested using EMTP simulation and real data records.

Keywords Disturbance records · Adaptive protection · Transmission lines · Autoreclosure · Fault location · Electrical arc · Fault resistance · Spectral analysis · Unsynchronized/synchronized sampling

Z. Radojević
Next-generation Power Technology Center, Myongji University, Yongin, Gyeonggi-Do, 449-728, Korea
e-mail: radojevic@ieee.org

V. Terzija (✉)
EPSRC Chair Professor in Power System Engineering, The University of Manchester, School of Electrical and Electronic Engineering, Ferranti Building B6, Sackville Street, PO Box 88, Manchester M60 1QD, UK
e-mail: vladimir.terzija@manchester.ac.uk
URL: http://www.eee.manchester.ac.uk/
URL: http://www.eee.manchester.ac.uk/profiles/index.aspx?ID=1163

1 Introduction

The development of microprocessor and communication technology significantly influenced the design of modern intelligent electronic devices (IEDs) used for overhead line protection and disturbance records analysis. On the other hand, the fault analysis and generally data management over IEDs, plays an important role not only for the accurate location of the fault occurred on a line, but also for detailed analysis of all relevant parameters describing the fault (fault type, fault nature, tower footing and arc resistances, etc.) Once the fault is precisely located, the line can be repaired and efficiently restored. In the past, a variety of fault location algorithms were introduced as either an add-on feature in intelligent electronic devices, or a stand-alone implementation in fault locators [1]. The so called "two port" algorithms that use quantities from both transmission line terminals usually lead to more accurate results. A drawback is that they need time synchronization by GPS systems or computational routines [2–4]. This paper presents a new algorithm for transmission line fault location and disturbance records analysis, using data from both line terminals, without time synchronization. It determines very accurately the fault location, and it calculates both the tower footing and arc resistances. From the existing literature, a numerical algorithm for fault location, which was designed as a pure fault locator, is presented in [5]. In this paper a new algorithm that also determines the arc and tower footing resistances will be presented. The availability of the arc and tower footing resistances is a significant improvement, offering new opportunities to improve the current practice of line protection.

The value of the arc resistance determines the fault nature (permanent or transient fault), which is the information necessary to block/release the autoreclosure. The calculated arc resistance can be used as a criterion for making a decision

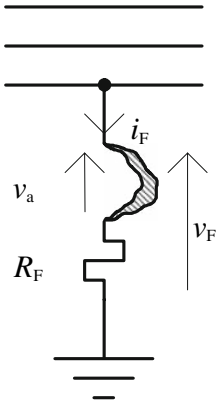

Fig. 1 Fault model including tower footing resistance and electrical arc

as to whether the fault is permanent or transient. The new algorithm is derived in the spectral domain using the widely used discrete fourier transformation (DFT) for phasor calculation. The results of the algorithm testing are presented, demonstrating the efficiency of the new algorithm.

Realistic fault modelling is a prerequisite for the design of an efficient algorithm for disturbance records analysis. The next section of this paper introduces a realistic fault model including both the tower footing and arc resistances.

2 Fault model

Approximately 70–90% of all faults on overhead lines are single line to ground arcing faults, so in this paper this type of fault will be analyzed. For this case the fault model can be represented as a series connection of an arc voltage v_a and a tower footing resistance R_F (see Fig. 1).

An arc is a source of harmonics, so realistic modelling must include the higher harmonics originating from the arc, or from other nonlinear sources existing in the system. The hth harmonic of the fault voltage can be expressed as follows:

$$\underline{V}_F^h = \underline{V}_a^h + R_F \underline{I}_F^h, \tag{1}$$

where $\underline{V}_a^h$ is the hth harmonic of the arc voltage v_a, and $\underline{I}_F^h$ is the hth harmonic of the fault current I_F. By this, the fundamental harmonic of the fault voltage becomes (for simplicity, here the superscript "1" is omitted):

$$\underline{V}_F = \underline{V}_a + R_F \underline{I}_F. \tag{2}$$

The fundamental harmonic of the arc voltage can be expressed as follows:

$$\underline{V}_a = \underline{k} V_{arc}, \tag{3}$$

where k is the first harmonic coefficient, and V_{arc} is the arc voltage amplitude [6]. Since the arc current and arc voltage are in phase, the following holds:

$$\underline{k} = k \angle \varphi, \tag{4}$$

where φ is the phase angle of the fundamental harmonic of the arc current:

$$\varphi = \arg\{\underline{I}_F\}. \tag{5}$$

The phasor of the arc voltage fundamental harmonic can be now expressed as follows:

$$\underline{V}_a = \underline{k}\, V_{arc} = k \angle \varphi\, V_{arc} = k \frac{\underline{I}_F}{|\underline{I}_F|} V_{arc} = R_a \underline{I}_F, \tag{6}$$

where

$$R_a = k \frac{V_{arc}}{|\underline{I}_F|} \tag{7}$$

is the arc fundamental harmonic resistance.

By combining Eqs. (1) and (6), one obtains the following fault model for the fundamental harmonic:

$$\underline{V}_F = R_T \underline{I}_F, \tag{8}$$

where

$$R_T = R_a + R_F \tag{9}$$

is the *total fault resistance*.

The same consideration of the fault model can be carried out for other higher harmonics. For the third harmonic it takes the following form (here the superscript 3 denotes the third harmonic):

$$\underline{V}_F^3 = \underline{V}_a^3 + R_F \underline{I}_F^3 = \underline{k}^3\, V_{arc} + R_F \underline{I}_F^3 = k^3 \angle 3\varphi\, V_{arc} + R_F \underline{I}_F^3, \tag{10}$$

where k^3 is the coefficient for the third harmonic. The last equation will be used in the part of the new algorithm in which the unknown arc resistance is determined.

3 Derivation of the New Numerical Algorithm

3.1 Fault location algorithm stage

Let us assume an a-phase single line to ground arcing fault on a transmission line at a distance ℓ, observed from the left line terminal, as presented in Fig. 2. Under the assumption that the line is short (e.g. lines at HV/MV level up to 100 km), the shunt capacitance and the shunt conductance of the transmission line can be neglected. In Fig. 2 all of the variables have radian frequency multiplied by the harmonics order h and all of the line parameters are calculated in terms of $(h\omega)$. At this stage of the algorithm development it is assumed that the variables on both line terminals are synchronized. The fault location is denoted by F and the fault distance by ℓ. The index h denotes the order of harmonic, D is line length, subscript S and R denote the sending- and receiving end of the line, respectively.

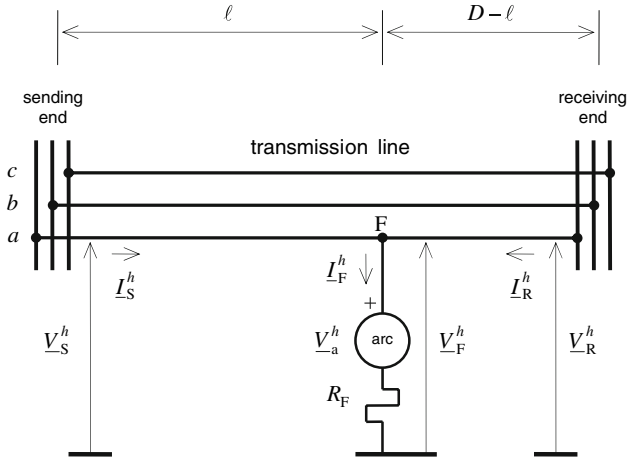

Fig. 2 Single line to ground arcing fault

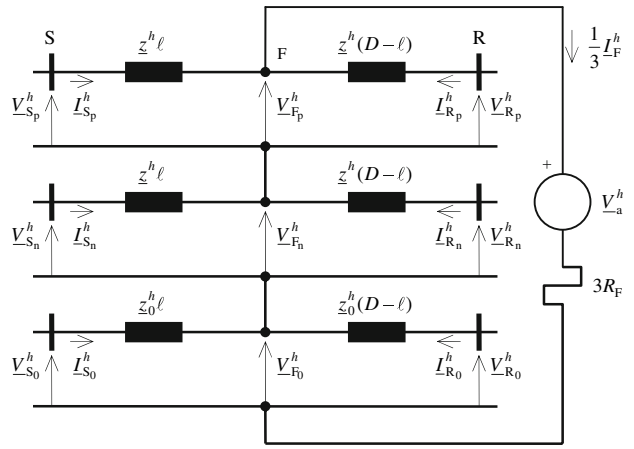

Fig. 3 Equivalent sequence network connection of faulted lines

Using the symmetrical components approach, the unsymmetrical three phase circuit from Fig. 3 can be represented by three single-phase equivalent circuits (positive (p), negative (n), and zero (0) sequence circuits, respectively), as shown in Fig. 3.

For the circuit from Fig. 3, the following holds:

$$\underline{V}^h_S = \underline{z}^h \left(\underline{I}^h_S + \underline{k}^h_z \underline{I}^h_{S_0}\right) \ell + \underline{V}^h_F, \tag{11}$$

$$\underline{V}^h_R = \underline{z}^h \left(\underline{I}^h_R + \underline{k}^h_z \underline{I}^h_{R_0}\right) (D-\ell) + \underline{V}^h_F, \tag{12}$$

where $\underline{k}^h_z = \frac{\underline{z}^h_0 - \underline{z}^h}{\underline{z}^h}$ is the zero sequence compensation factor, which depends on the line parameters and which can be calculated in advance; $\underline{V}^h_{S_{p,n,0}}$, $\underline{V}^h_{R_{p,n,0}}$ are the hth harmonics of positive-, negative-, and zero sequence phase voltage at both ends of the lines (S—sending, and R—receiving end); $\underline{I}^h_{S_{p,n,0}}$, $\underline{I}^h_{R_{p,n,0}}$ are the hth harmonics of the positive-, negative-, and zero sequence phase current at both ends of the lines; $\underline{V}^h_{F_{p,n,0}}$ are the hth harmonics of the positive-, negative-, and zero sequence faulted phase voltage at the fault point; $\underline{z}^h$ are positive- or negative sequence line impedances for the hth harmonic, $\underline{z}^h_0$ is the zero sequence line impedance for the hth harmonic.

Equation (11), rewritten for the fundamental harmonic, becomes:

$$\underline{V}_F = \underline{V}_S - \underline{z}(\underline{I}_S + \underline{k}_z \underline{I}_{S_0})\ell. \tag{13}$$

Let us now assume that terminal variables are not synchronized. That means that for both terminals two different coordinate systems can be assigned: one for the sending and one for the receiving line terminal. Thus, for the receiving end line terminal, the following equation, derived from Eq. (12) and rewritten for the fundamental harmonic, can be derived:

$$\underline{V}^*_F = \underline{V}^*_R - \underline{z}(\underline{I}^*_R + \underline{k}_z \underline{I}^*_{R_0})(D-\ell). \tag{14}$$

Here the superscript "*" denotes that phasors from Eq. (14) are not synchronized with phasors from Eq. (13). From Eqs. (13) and (14), the fault distance ℓ, and the total fault resistance R_T can be calculated.

Based on the fact that the amplitudes of the fault voltages from Eqs. (13) and (14) are the same, as indicated in [5], the following holds:

$$\left|\underline{V}_F\right| = \left|\underline{V}^*_F\right|. \tag{15}$$

By combining Eqs. (13)–(15), one obtains:

$$\left|\underline{V}_S - \underline{z}(\underline{I}_S + \underline{k}_z \underline{I}_{S_0})\ell\right| = \left|\underline{V}^*_R - \underline{z}(\underline{I}^*_R + \underline{k}_z \underline{I}^*_{R_0})(D-\ell)\right|. \tag{16}$$

By separating real and imaginary terms in the complex Eq. (16), the following equation can be obtained:

$$|(a + b\cdot\ell) + j(c + d\cdot\ell)| = |(e + f\cdot\ell) + j(g + h\cdot\ell)|, \tag{17}$$

where

$$\begin{aligned}
a &= \mathrm{Re}(\underline{V}_S), \quad b = -\mathrm{Re}[\underline{z}(\underline{I}_S + \underline{k}_z \underline{I}_{S_0})],\\
c &= \mathrm{Im}(\underline{V}_S), \quad d = -\mathrm{Im}[\underline{z}(\underline{I}_S + \underline{k}_z \underline{I}_{S_0})],\\
e &= \mathrm{Re}[\underline{V}^*_R - \underline{z}(\underline{I}^*_R + \underline{k}_z \underline{I}^*_{R_0})D], \quad f = \mathrm{Re}[\underline{z}(\underline{I}^*_R + \underline{k}_z \underline{I}^*_{R_0})],\\
g &= \mathrm{Im}[\underline{V}^*_R - \underline{z}(\underline{I}^*_R + \underline{k}_z \underline{I}^*_{R_0})D], \quad h = \mathrm{Im}[\underline{z}(\underline{I}^*_R + \underline{k}_z \underline{I}^*_{R_0})].
\end{aligned}$$

From (17) one obtains:

$$(a + b\cdot\ell)^2 + (c + d\cdot\ell)^2 = (e + f\cdot\ell)^2 + (g + h\cdot\ell)^2. \tag{18}$$

Equation (18) can be rewritten as follows:

$$\ell^2 + p\ell + q = 0, \tag{19}$$

where

$$p = \frac{2(ab + cd - ef - gh)}{b^2 + d^2 - f^2 - h^2}, \quad \text{and} \quad q = \frac{a^2 + c^2 - e^2 - g^2}{b^2 + d^2 - f^2 - h^2}.$$

Equation (19) is a quadratic equation with two solutions:

$$\ell_{1/2} = \frac{-p \pm \sqrt{p^2 - 4q}}{2}. \tag{20}$$

Using Eq. (20), two cases can occur: (a) one solution in the range 0–D and a second solution outside of this interval and (b) both solutions in the range 0–D. In case (a), the first solution is the exact one. In case (b), an additional procedure must be applied to determine the exact solution. Thus, the problem appears if both solutions are positive values and in the range of 0–D. In these cases the selection of the true fault location can be achieved by analyzing the equivalent zero-sequence equivalent circuit, which gives two new solutions. One of them is equal to one of two solutions obtained from the positive sequence equivalent circuit and this is the true unknown fault location.

By this, the fault location stage of the algorithm is accomplished.

3.2 Total fault resistance algorithm stage

From the calculated fault location, the voltage at the location of the fault can be determined:

$$\underline{V}_{\mathrm{F}} = \underline{V}_{\mathrm{S}} - \underline{z}(\underline{I}_{\mathrm{S}} + \underline{k}_{\mathrm{z}}\underline{I}_{\mathrm{S}_0})\ell. \tag{21}$$

Based on the assumed model, for which it is valid that $\underline{V}_{\mathrm{F}} = R_{\mathrm{T}}\underline{I}_{\mathrm{F}}$, it can be concluded that

$$\arg(\underline{I}_{\mathrm{F}}) = \arg(\underline{V}_{\mathrm{F}}). \tag{22}$$

The phase difference between the sending end current and the fault current is given as follows:

$$\theta = \arg(\underline{I}_{\mathrm{S}}) - \arg(\underline{I}_{\mathrm{F}}). \tag{23}$$

By this, the RMS of the fault current becomes:

$$\left|\underline{I}_{\mathrm{F}}\right| = \left|\underline{I}_{\mathrm{S}}\right|\cos(\theta) + \sqrt{(I_{\mathrm{R}}^{*})^2 - [\left|\underline{I}_{\mathrm{S}}\right|\cos(\theta)]^2}. \tag{24}$$

Finally, the total fault resistance can be expressed as follows:

$$R_{\mathrm{T}} = \frac{\left|\underline{V}_{\mathrm{F}}\right|}{\left|\underline{I}_{\mathrm{F}}\right|}. \tag{25}$$

By this, the total fault resistance stage of the algorithm is accomplished.

3.3 Arc resistance algorithm stage

Based on the expressions for the fault distance and total fault resistance and by using the fault model equation for third harmonics, the unknown arc and tower footing resistances can be determined.

From Eq. (11) written for the third harmonics, the third harmonic of the voltage at the fault location can be calculated:

$$\underline{V}_{\mathrm{F}}^3 = \underline{V}_{\mathrm{S}}^3 - \underline{z}^3\left(\underline{I}_{\mathrm{S}}^3 + \underline{k}_{\mathrm{z}}^3\underline{I}_{\mathrm{S}_0}^3\right)\ell. \tag{26}$$

By assuming that the zero sequence equivalent circuit is a purely passive one, the following holds:

$$\underline{I}_{\mathrm{F}}^3 = c\underline{I}_{\mathrm{S}_0}^3, \tag{27}$$

where c is a real constant number. Its value must not be known in advance. By combining Eqs. (27) and (10), one obtains:

$$\underline{V}_{\mathrm{F}}^3 = \underline{k}^3 V_{\mathrm{arc}} + R_{\mathrm{Fe}}\underline{I}_{\mathrm{S}_0}^3, \tag{28}$$

where $R_{\mathrm{Fe}} = cR_F$.

By putting Eq. (7) into Eq. (28), one obtains:

$$\underline{V}_{\mathrm{F}}^3 = \underline{k}^3\frac{\left|\underline{I}_{\mathrm{F}}\right|}{k}R_a + R_{\mathrm{Fe}}\underline{I}_{\mathrm{S}_0}^3. \tag{29}$$

From (29) the following equation can be derived:

$$R_{\mathrm{Fe}} = \frac{\underline{V}_{\mathrm{F}}^3}{\underline{I}_{\mathrm{S}_0}^3} - \frac{\underline{k}^3}{\underline{I}_{\mathrm{S}_0}^3}\frac{\left|\underline{I}_{\mathrm{F}}\right|}{k}R_{\mathrm{a}}. \tag{30}$$

The imaginary part of the left hand side of Eq. (30) is equal to zero, so the imaginary part of the right hand side must be zero, too. From this, one obtains:

$$\mathrm{Im}(R_{\mathrm{Fe}}) = \mathrm{Im}\left(\frac{\underline{V}_{\mathrm{F}}^3}{\underline{I}_{\mathrm{S}_0}^3} - \frac{\underline{k}^3}{\underline{I}_{\mathrm{S}_0}^3}\frac{\left|\underline{I}_{\mathrm{F}}\right|}{k}R_{\mathrm{a}}\right) = 0. \tag{31}$$

From the last equation the following can be obtained:

$$\mathrm{Im}\left(\frac{\underline{V}_{\mathrm{F}}^3}{\underline{I}_{\mathrm{S}_0}^3}\right) - \left[\frac{\left|\underline{I}_{\mathrm{F}}\right|}{k}\mathrm{Im}\left(\frac{\underline{k}^3}{\underline{I}_{\mathrm{S}_0}^3}\right)\right]R_{\mathrm{a}} = 0. \tag{32}$$

Equation (32) gives the explicit equation for the unknown arc resistance:

$$R_{\mathrm{a}} = \frac{k}{\left|\underline{I}_{\mathrm{F}}\right|}\cdot\frac{\mathrm{Im}\left(\frac{\underline{V}_{\mathrm{F}}^3}{\underline{I}_{\mathrm{S}_0}^3}\right)}{\mathrm{Im}\left(\frac{\underline{k}^3}{\underline{I}_{\mathrm{S}_0}^3}\right)}. \tag{33}$$

The tower footing resistance R_{F} can be simply calculated as:

$$R_{\mathrm{F}} = R_{\mathrm{T}} - R_{\mathrm{a}}. \tag{34}$$

Using the method described, for arcless (metallic) faults it is expected that $R_{\mathrm{T}} = R_{\mathrm{F}}$ and $R_{\mathrm{a}} = 0$. This is proved in the next section of the paper through computer tests.

Based on the arc resistance determined by the algorithm presented, the fault nature (transient or permanent fault) can be recognized as well. This information can be very useful used for blocking the autoreclosing procedure. If the fault is a permanent (arcless) fault, the autoreclosure should be blocked; on the contrary, if the fault is a transient (arcing) fault, it should be released.

The algorithm presented assumes the use of unsynchronized phasors measured at remote line terminals. The algorithm could be also used if the phasors are synchronized, i.e. if the facilities for phasor synchronization are available. Under

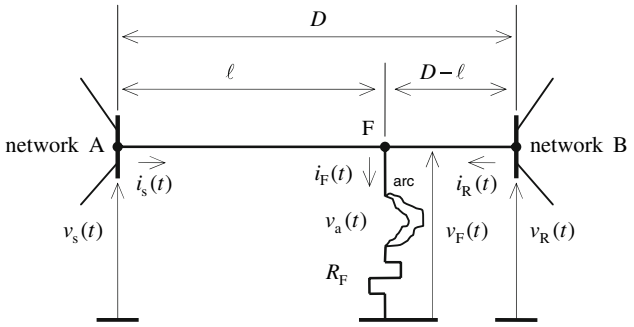

Fig. 4 Single line diagram of the simulated test power system

these circumstances, the loss of synchronization should not affect the algorithm, since it does not require the synchronization.

4 Computer simulated tests

The validity of the algorithm was tested by using The electromagnetic transient program [7] developed for the investigation of arcing phenomena in power systems. In Fig. 4 a schematic diagram of a 400 kV test power system is presented.

In Fig. 4, variables $v_S(t)$, $v_R(t)$, $i_S(t)$ and $i_R(t)$ denote the synchronized sampled voltages and currents, whereas $D = 100\,\text{km}$, $r = 0.0325\,\Omega/\text{km}$, $x = 0.3\,\Omega/\text{km}$, $r_0 = 0.0975\,\Omega/\text{km}$, and $x_0 = 0.9\,\Omega/\text{km}$ represent the line parameters. Data for network A were: $R_A = 2\,\Omega$, $L_A = 0.1\,\text{H}$, $R_{A0} = 4.\,\Omega$ and $L_{A0} = 0.2\,\text{H}$. Data for network B were: $R_B = 1.28\,\Omega$, $L_B = 0.064\,\text{H}$, $R_{B0} = 2.54\,\Omega$ and $L_{B0} = 0.128\,\text{H}$. The equivalent electromotive force of networks A and B were respectively $E_A = 416\,\text{kV}$ and $E_B = 400\,\text{kV}$.

Single line to ground arcing faults are simulated at different locations on the overhead line. The pre-fault load existed before the fault.

In the following test example, a single phase fault, simulated at the 10th km observed from the left line terminal, is analyzed. The simulation was carried out with the time step corresponding to the sampling frequency $f_s = 3{,}200\,\text{Hz}$ (64 sample/T_0).

The first simulation was performed by assuming that the arc voltage has a square wave waveform with an amplitude of $V_a = 4\,\text{kV}$ and with typical arc ignition and quenching distortions (see Fig. 5). The value of 4 kV was obtained under the assumption that the distance between the arc horns in questions is $L_i = 3.25\,\text{m}$ and that the arc voltage gradient inside the arc column is $E_a = 1{,}250\,\text{V/m}$. The fault inception was at $t = 20\,\text{ms}$ and the tower footing resistance was $R_F = 8\,\Omega$. In the example given, a synchronization error of 90° in the phase of the input data acquired from the remote terminal was assumed.

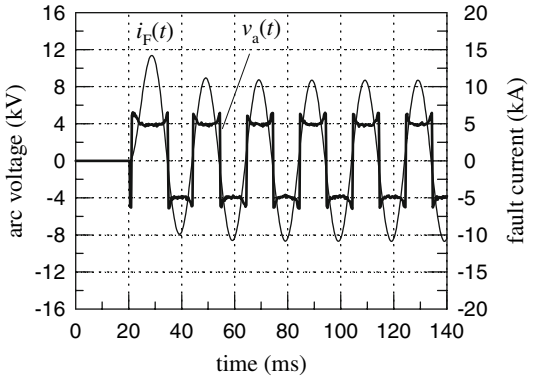

Fig. 5 Arc voltage and fault current

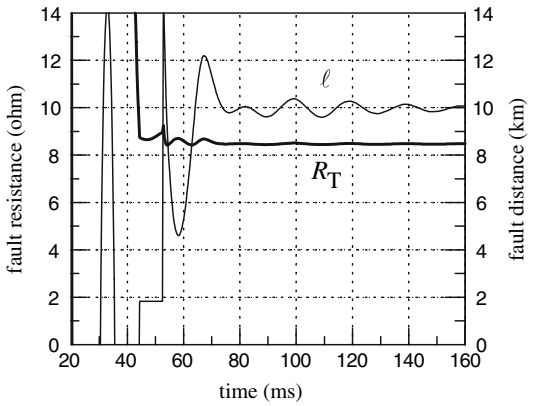

Fig. 6 Fault distance and total fault resistance (arcing fault)

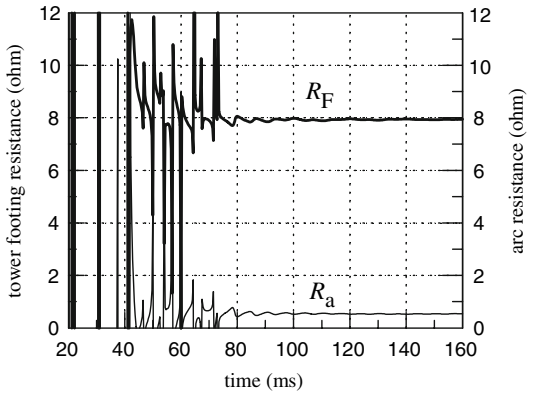

Fig. 7 Tower footing and arc resistances (arcing fault case)

In Figs. 6 and 7 the results obtained using the algorithm are given. Figure 6 shows the values of fault location and total fault resistance, while Fig. 7 shows both the arc and the tower footing resistances. Obviously, when adding the arc and the tower footing resistances, one obtains the total fault resistance.

In the next example an arcless fault is simulated with the total fault resistance of 8Ω and fault distance of 10 km. Figure 8 shows very accurate results obtained using the

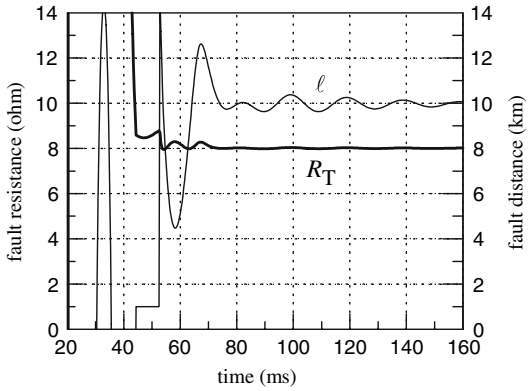

Fig. 8 Fault distance and total fault resistance (arcless fault case)

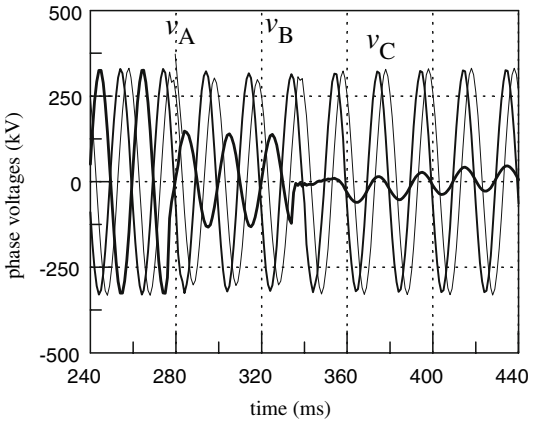

Fig. 9 Input voltages measured by the relay at the sending end

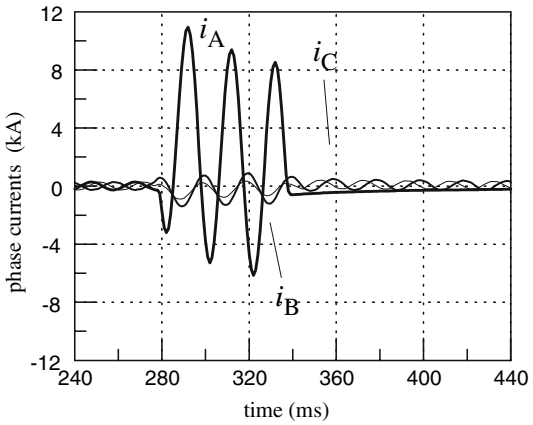

Fig. 10 Input currents measured by the relay at the sending end

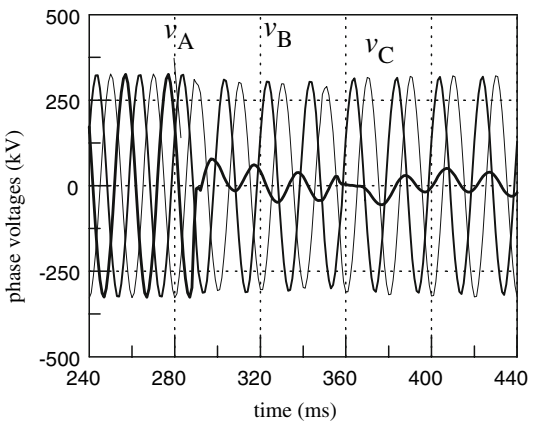

Fig. 11 Input voltages measured by the relay at the receiving end

proposed algorithm. The arc resistance value $R_a = 0\,\Omega$ is obtained, which actually corresponds to a metallic (permanent) fault.

The algorithm features are also derived in the following cases: fault location varied in the range 1–99 km; tower footing resistance varied in the range 0–100 Ω ; synchronisation error varied in the range 1–360°; arc voltage amplitude varied in the range 0–10 kV. Under all of the above described circumstances, the unknowns are accurately obtained.

The presented algorithm can be implemented in real-time (e.g. distance protection and adaptive autoreclosing), or in an off-line mode (e.g. fault location and fault analysis). For a real-time application the speed of the algorithm, communication delays, and the real-time data acquisition time are important factors. The algorithm convergence properties are determined by the fault angle and the selection of the data window size. Based on the results obtained (e.g. Fig. 7), the worst cases of algorithm convergence are observed to be approximately 50–60 ms. This is still acceptable for performing autoreclosure. Note that the fault nature (arcing or metallic fault) must be identified before circuit breaker opening. For an off-line application the convergence is not a key issue.

5 Field testing

In order to check the validity of the algorithm presented, voltages and currents, recorded during faults on a real 400 kV, 82 km long transmission line, are processed. Here, a typical example of an arcing fault will be analyzed. In Figs. 9, 10, 11 and 12, voltages and currents, measured by the relay before and during a single-phase line to ground arcing fault, are presented respectively. All of the signals are sampled with the sampling frequency $f_s = 1,000$ Hz. From Figs. 10 and 12 it is obvious that the fault that occurred was a single line to ground fault. It was selectively tripped by the line protection. In this particular case, only the faulted phase was tripped.

Voltages and currents, recorded and stored in Comtrade format, are processed using the algorithm presented. In the algorithm, the data window length was set to $T_{dw} = 20$ ms. The results obtained are presented in Figs. 13, 14 and 15 respectively. The unknown fault location $\ell = 41.2$ km was obtained (see Fig. 13). Based on the assessment of the recorded fault record and result obtained by the installed

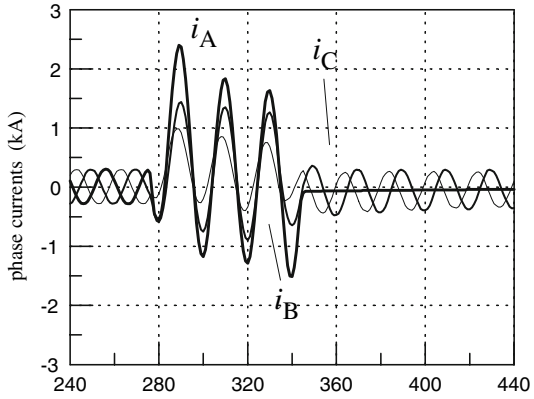

Fig. 12 Input currents measured by the relay at the receiving end

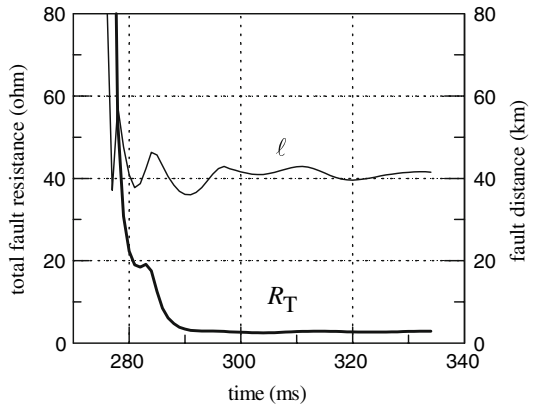

Fig. 13 Calculated fault distance and total fault resistance

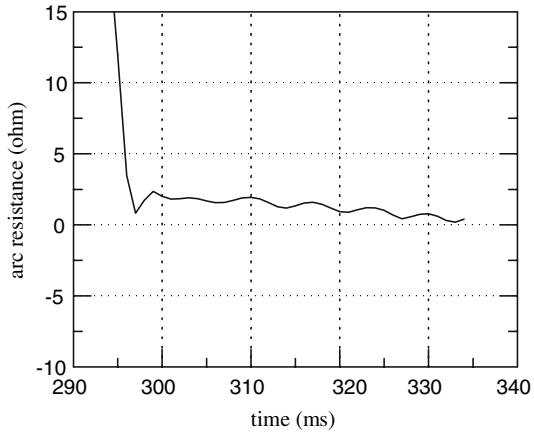

Fig. 14 Calculated arc resistance

distance protection, a reasonable agreement between the results obtained is achieved. The result obtained using the existing distance relay was 5% larger. The reason for this mismatch lies in the fact that distance protection does not take into account the fault resistance, and sees the fault point as further away than the true one. In Fig. 13 the total fault resistance is depicted, too.

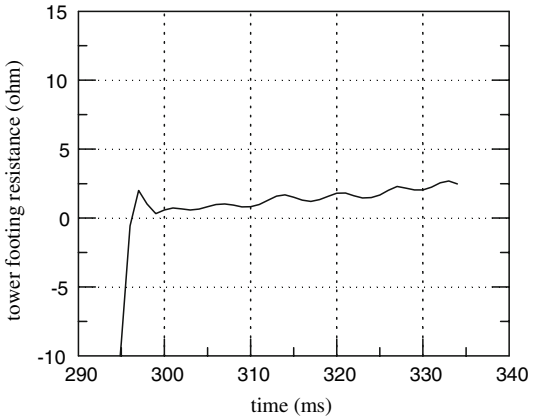

Fig. 15 Calculated tower footing resistance

In Fig. 14 the unknown arc resistance is presented. Obviously, an arc resistance larger than zero, is obtained. That means that the case analyzed was an arcing fault. As it can be observed, the arc voltage resistance is on average approximately 0.5 Ω. In Fig. 15 the unknown tower footing resistance is presented. Its value is relatively small, which matches the statistical values obtained in this season of the year.

The results obtained by the processing of real data confirm the high quality of the algorithm presented. The significance of the algorithm is improved accuracy and reduced hardware requirements—there is no need for the synchronization of data sampling between remote line terminals.

6 Conclusions

This paper presents a new spectral domain numerical algorithm for overhead lines protection and disturbance records analysis. The algorithm does not require synchronization of data sampled at remote line terminals. The algorithm can be also used in all schemes in which the synchronized measurement is assumed, or if it is not precise enough. Through realistic fault modelling and by introducing a new model of the electrical arc, compared to approaches that do not take the arc into consideration, the higher accuracy of the fault location is achieved. In addition, a new method of blocking/releasing autoreclosure, based on the calculated arc resistance, has been proposed and successfully tested. It is shown that the algorithm is not sensitive to values of tower footing resistance and fault location (close in, or remote faults). Using transient simulations, both the arcing and arcless faults are thoroughly tested and analyzed. Accurate results are achieved in determining all unknowns: the fault location, arc resistance, tower footing resistance and fault nature. The validation of the proposed algorithm using real data presents a particular encouragement for the successful future implementation of the algorithm presented.

Acknowledgment This work was supported by the ERC program of MOST/KOSEF (Next-generation Power Technology Center).

References

1. Sidhu TS et al (2006) Bibliography of relay literature, 2003 IEEE committee report. IEEE Trans Power Deliv 21:56–65
2. Johns AT, Jamali S (1990) Accurate fault location technique for power transmission line. IEE Proc 137:395–402
3. Novosel D, Hart DG, Udren E, Garitty J (1992) Unsynchronized two-terminal fault location estimation. IEEE Trans Power Deliv 7(1):98–107
4. Girgis AA, Hart DG, Peterson WL (1992) A new fault location technique for two-and three-terminal lines. IEEE Trans Power Deliv 7(1):98–107
5. Silveira EG, Pereira C (2007) Transmission line fault location using two-terminal data without time synchronization. IEEE Trans Power Syst 22(1):498–499
6. Djurić M, Terzija V (1995) A new approach to the arcing faults detection for autoreclosure in transmission systems. IEEE Trans Power Deliv 10(4):1793–1798
7. Lönard D, Simon R, Terzija V (1992) Simulation von Netzmodellen mit zweiseitiger Einspeisung zum Test von Netzschutzeinrichtungen. TB-157/92 Univ. Kaiserslautern (in German)